ARKIV FÖR FYSIK Band 19 nr 16

Communicated 11 January 1961 by B. Edlén and E. Rudberg

The spectrum of the neutral nitrogen atom in the lead-sulfide region

By Karl Börje S. Eriksson and Ingmar Johansson

With 1 figure in the text

SUMMARY

In the spectrum of the neutral nitrogen atom, N I, wavelengths have been determined for 113 lines in the region 18751–11998 Å by using a scanning spectrograph with a Kodak Ektron detector and modulated radiation sources, viz. a hollow cathode and an electrodeless discharge. A system of accurately connected energy levels, including the complete configurations $2p^3$, $2p^4$, $3s$, $4s$, $5s$, $3d$, and $4f$, has been derived. A number of infrared intercombination lines fix the doublet and quartet systems in relation to each other; the laboratory data confirm Bowen's measurements of forbidden N I lines in nebular spectra. The empirically established $4f$ levels have been found to follow the formulae for intermediate pair coupling. With the support of theory some $5f$ levels have also been determined.

Introduction

In an earlier investigation of N I in the photographic region accurate values were determined for a group of 29 quartet levels and for an other group of 25 doublet levels (Eriksson, 1958*a*). Some levels of $3d\ ^2F$ and $3d\ ^2D$ were tied to the quartet system by intercombination lines, but combinations between these $3d$ doublet levels and the $3p$ doublet levels were not observed, as they would fall in the infrared beyond the sensitivity limit of photographic emulsions. The main object of the present investigation was to measure these doublet combinations by means of a lead-sulfide spectrograph and thereby obtain an accurate connection between the doublet and the quartet systems. Other intercombination lines could also be expected in the same region of the spectrum, as well as lines originating in the transitions $3d$–nf. The only previous measurements on nitrogen lines in this region are those by Ingram (1929) with an estimated wavelength accuracy of 2 Å. His radiation source was a carbon arc in air with a current of 125 A.

The experimental equipment

Radiation sources

The observations started in 1958 with a hollow-cathode discharge as a light source. In order to increase the radiation output the equipment was modified several times.

The final design consisted of a water-cooled, 11 cm long, open-ended, iron cylinder with an inner diameter of 12 mm. The arrangement was cylindrically symmetric with one cylindric anode at each end of the cathode, insulated from the cathode by means of porcelain plates. The joints were made vacuum-tight by means of O-rings. A quartz window was attached to the open end of each anode by means of vacuum grease. A spherical concave mirror was placed behind the light source in order to reflect the backward emerging light back through the hollow cathode toward the spectrograph. The discharge tube was fed with an unsmoothed, full-wave-rectified current from a high-voltage transformer. Thus, the lead-sulfide cell was irradiated by intermittent light, and no further modulation of the light was necessary for the purpose of amplification. The discharge was run in a mixture of helium and neon with an admixture of 20–30 % nitrogen, the total pressure being about 1 mm Hg. The maximum effective value of the current was 2.5 A, and the voltage across the tube was about 500 V.

With the aid of this light source 12 lines between 15771 Å and 12461 Å were measured. These measurements[1] established the wanted connection between the doublet and quartet systems. A few more lines were observed in regions where the background of molecular bands was troublesome, but the transitions $3d$–$4f$ could not be found.

When the observations were resumed in 1959 we employed an electrodeless high-frequency discharge similar to the one used in Eriksson's photographic investigation (Eriksson, 1958*a*; Minnhagen and Stigmark, 1954). The discharge tube, of fused quartz, was 20 cm long. The central part had a diameter of 20 mm, while the ends of the tube were conically enlarged. To the ends were fused plane quartz windows of 40 mm diameter. Two side tubes connected the discharge tube to a gas-circulating system. The tube was surrounded by the coil of a high-frequency circuit, link-coupled to a 18 MHz generator. An anode voltage of 4.5–5.5 kV was used for the power amplifier tube (Philips QB 3.5/750). The high-frequency current was pulsed to 100 Hz, the pulse length being 1.2 msec. With an anode voltage of 5.5 kV the average power supplied to the discharge tube amounted to about 0.3 kW, corresponding to a peak power of about 2.5 kW. The frequency of the light pulses were used as amplifying frequency for the current through the photoresistor.

The method of photoelectric recording is particularly well suited to adjust the equipment for optimum radiation conditions. After setting on a suitable spectral line the composition and pressure of the gas, and the voltage etc. are varied until maximum signal is obtained. The most favourable gas mixture consisted of neon at a partial pressure of 0.7 mm Hg and nitrogen at a partial pressure of 0.07 mm Hg.

The lines previously observed with the hollow cathode came out considerably stronger with the high-frequency discharge, and several new atomic lines, particularly in the short-wave region, grew up from the background of molecular bands. From 18751 Å to 17220 Å about 40 new lines were found, which proved to be due to $3d$–$4f$ transitions.

The spectrograph

The spectrum was recorded by means of a Pfund-type scanning spectrograph with a Kodak Ektron photo-resistor. The spectrograph has been briefly described by Johansson (1959). Two different gratings were used, one with 46000 grooves

---

[1] Briefly described at the Conference of the Swedish National Committee for Physics in 1959. [Arkiv Fysik 16, 490 (1960).]

Table 1. N I lines in the region 18 751 Å to 11 998 Å.

Abbreviations: bl = blended by molecular band; ul = unsymmetrical, shaded to longer waves; us = unsymmetrical, shaded to shorter waves; * = measured also with a hollow cathode; ** = predicted value.

Intensity	Wavelength, Å		Wave-number, cm⁻¹		Combination
	This work	Ingram	Obs.	Calc.	
2	18 751.01		5331.59	1.57 1.49	$3d\,^4D_{7/2}-4f\,D(3)_{7/2}$ $^4D_{7/2}-\ D(3)_{5/2}$
4	18 670.00		5354.72	4.71 4.72	$^2D_{5/2}-\ F(3)_{7/2}$ $^2D_{5/2}-\ F(3)_{5/2}$
32	18 658.16		5358.12	8.12	$^2D_{5/2}-\ F(4)_{7/2}$
13	18 630.19		5366.17	6.16 6.08	$^2D_{3/2}-\ F(2)_{5/2}$ $^2D_{3/2}-\ F(2)_{3/2}$
13	18 587.24		5378.57	8.55	$^2D_{3/2}-\ F(3)_{5/2}$
4	18 566.75		5384.50	4.49 4.58	$^4D_{7/2}-\ G(4)_{9/2}$ $^4D_{7/2}-\ G(4)_{7/2}$
11	18 251.58		5477.48	7.49 7.41	$^4D_{5/2}-\ F(2)_{5/2}$ $^4D_{5/2}-\ F(2)_{3/2}$
13	18 240.54		5480.80	0.82 0.83	$^4D_{7/2}-\ F(3)_{7/2}$ $^4D_{7/2}-\ F(3)_{5/2}$
60	18 229.66		5484.07	4.08 4.23	$^4D_{7/2}-\ F(4)_{9/2}$ $^4D_{7/2}-\ F(4)_{7/2}$
32 ul	18 210.56		5489.82	9.87 9.88 9.77 9.69	$^4D_{5/2}-\ F(3)_{7/2}$ $^4D_{5/2}-\ F(3)_{5/2}$ $^4D_{3/2}-\ F(2)_{5/2}$ $^4D_{3/2}-\ F(2)_{3/2}$
8	18 199.13		5493.27	3.28	$^4D_{5/2}-\ F(4)_{7/2}$
13	18 171.60		5501.59	1.59	$^4D_{1/2}-\ F(2)_{3/2}$
13	18 169.74		5502.15	2.16	$^4D_{3/2}-\ F(3)_{5/2}$
6	18 116.27		5518.39	8.40	$^4P_{1/2}-\ D(2)_{3/2}$
12	18 108.61		5520.73	0.74 0.83	$^2F_{7/2}-\ G(4)_{9/2}$ $^2F_{7/2}-\ G(4)_{7/2}$
10	18 097.71		5524.05	4.06 3.98	$^4P_{5/2}-\ D(3)_{7/2}$ $^4P_{5/2}-\ D(3)_{5/2}$
33 ul	18 049.56		5538.79	8.81 8.73 f'	$^2F_{5/2}-\ D(3)_{7/2}$ $^2F_{5/2}-\ D(3)_{5/2}$ $3d'\,^2G\ -4f'\,H(5)$
30	18 029.95		5544.81	4.82 4.77	$3d\,^4P_{3/2}-4f\,D(2)_{5/2}$ $^4P_{3/2}-\ D(2)_{3/2}$
51	17 979.89		5560.25	0.25 0.18	$^4P_{5/2}-\ G(3)_{7/2}$ $^4P_{5/2}-\ G(3)_{5/2}$
17	17 936.55		5573.69	3.69	$^4P_{1/2}-\ D(1)$
8	17 925.70		5577.06	7.07	$^4P_{5/2}-\ G(4)_{7/2}$
7	17 918.06		5579.44	9.44 9.39	$^4P_{5/2}-\ D(2)_{5/2}$ $^4P_{5/2}-\ D(2)_{3/2}$
100	17 878.26		5591.86	1.89 1.82	$^2F_{7/2}-\ G(5)_{9/2}$ $^2F_{5/2}-\ G(4)_{7/2}$
10	17 852.09		5600.06	0.06	$^4P_{3/2}-\ D(1)$
8 us	17 787.27		5620.46	0.48 0.33	$^2F_{7/2}-\ F(4)_{7/2}$ $^2F_{7/2}-\ F(4)_{9/2}$
42	17 643.98		5666.11	6.11 6.03	$^4F_{5/2}-\ D(3)_{7/2}$ $^4F_{5/2}-\ D(3)_{5/2}$
8	17 636.83		5668.41	8.41 8.34	$^4F_{7/2}-\ G(3)_{7/2}$ $^4F_{7/2}-\ G(3)_{5/2}$

Table 1 (cont.)

Intensity	Wavelength, Å		Wave-number, cm^{-1}		Combination
	This work	Ingram	Obs.	Calc.	
100 ul	17 584.86		5685.16	5.14	$3d\ ^4F_{7/2}-4f\ G(4)_{9/2}$
				5.23	$^4F_{7/2}-\ G(4)_{7/2}$
				4.96	$^4F_{3/2}-\ D(3)_{5/2}$
18	17 531.99		5702.30	2.30	$^4F_{5/2}-\ G(3)_{7/2}$
				2.23	$^4F_{5/2}-\ G(3)_{5/2}$
125 us	17 516.58		5707.32	*f*	$^4F_{9/2}-\ G(5)_{11/2}$
				7.47	$^4F_{9/2}-\ G(5)_{9/2}$
27	17 480.41		5719.13	9.12	$^4F_{5/2}-\ G(4)_{7/2}$
32	17 474.16		5721.17	1.16	$^4F_{3/2}-\ G(3)_{5/2}$
24	17 436.22		5733.62	3.62	$^2P_{3/2}-\ D(3)_{5/2}$
16 us	17 429.23		5735.92	5.91	$^4F_{9/2}-\ F(4)_{9/2}$
				6.04	$^4F_{9/2}-\ F(4)_{7/2}$
12	17 385.13		5740.47	0.47	$^2P_{1/2}-\ D(2)_{3/2}$
23	17 367.55		5756.29	6.29	$^4F_{7/2}-\ G(5)_{9/2}$
16	17 326.86		5769.81	9.82	$^2P_{3/2}-\ G(3)_{5/2}$
6	17 291.81		5781.50	1.47	$^4F_{7/2}-\ F(3)_{7/2}$
				1.48	$^4F_{7/2}-\ F(3)_{5/2}$
4	17 282.04		5784.77	4.73	$^4F_{7/2}-\ F(4)_{9/2}$
				4.88	$^4F_{7/2}-\ F(4)_{7/2}$
11	17 269.17		5789.08	9.08	$^2P_{3/2}-\ D(2)_{5/2}$
				9.03	$^2P_{3/2}-\ D(2)_{3/2}$
10	17 219.55		5805.77	5.76	$^2P_{1/2}-\ D(1)$
22	15 771.10*	70.7	6338.98	8.98	$3p\ ^2P_{3/2}-4s\ ^2P_{1/2}$
54	15 682.86*	83.8	6374.65	4.64	$^2P_{1/2}-\ ^2P_{1/2}$
200	15 582.27*	82.3	6415.80	5.79	$^2P_{3/2}-\ ^2P_{3/2}$
34	15 496.13*	93.5	6451.46	1.45	$^2P_{1/2}-\ ^2P_{3/2}$
75	15 146.66	45.7	6600.31	0.31	$2p^4\ ^4P_{1/2}-3p\ ^4D_{1/2}$
26	15 102.29		6619.70	9.71	$^4P_{3/2}-\ ^4D_{1/2}$
75	15 094.96	92.8	6622.92	2.92	$^4P_{1/2}-\ ^4D_{3/2}$
80	15 050.88	50.1	6642.31	2.32	$^4P_{3/2}-\ ^4D_{3/2}$
180	14 966.60	65.4	6679.72	9.72	$^4P_{3/2}-\ ^4D_{5/2}$
15	14 952.07		6686.21	6.23	$^4P_{5/2}-\ ^4D_{3/2}$
100	14 868.87	66.5	6723.62	3.63	$^4P_{5/2}-\ ^4D_{5/2}$
300	14 757.07	55.7	6774.56	4.56	$^4P_{5/2}-\ ^4D_{7/2}$
55	14 681.04	81.1	6809.64	9.63	$3p\ ^2P_{3/2}-3d\ ^2P_{3/2}$
27	14 604.64	99.2	6845.27	5.29	$^2P_{1/2}-\ ^2P_{3/2}$
17	14 598.42		6848.18	8.19	$^2P_{3/2}-\ ^2P_{1/2}$
20	14 548.55		6871.66	1.67	$3p\ ^4S_{3/2}-4s\ ^4P_{1/2}$
36	14 522.81	20.8	6883.84	3.85	$3p\ ^2P_{1/2}-3d\ ^2P_{1/2}$
29	14 454.62		6916.31	6.32	$3p\ ^4S_{3/2}-4s\ ^4P_{3/2}$
80	14 313.21	13.0	6984.64	4.64	$^4S_{3/2}-\ ^4P_{5/2}$
14	13 686.03		7304.73	4.74	$2p^4\ ^4P_{1/2}-3p\ ^4P_{1/2}$
65	13 668.60	66.6	7314.04	4.04	$3p\ ^2P_{3/2}-3d\ ^2D_{3/2}$
60	13 651.63	49.3	7323.13	3.12	$2p^4\ ^4P_{1/2}-3p^4\ P_{3/2}$
58	13 649.74		7324.14	4.14	$^4P_{3/2}-\ ^4P_{1/2}$
350	13 624.18*	22.9	7337.88	7.87	$3p\ ^2P_{3/2}-3d\ ^2D_{5/2}$
35	13 615.56		7342.53	2.52	$2p^4\ ^4P_{3/2}-3p\ ^4P_{3/2}$
190	13 602.27*	01.6	7349.71	9.70	$3p\ ^2P_{1/2}-3d\ ^2D_{3/2}$

Table 1 (cont.)

Intensity	Wavelength, Å		Wave-number, cm⁻¹		Combination
	This work	Ingram	Obs.	Calc.	
115	13 588.55*		7357.12	7.14	$3p\ ^2D_{3/2}-4s\ ^2P_{1/2}$
200	13 587.73*		7357.57	7.58	$^2D_{5/2}-\quad ^2P_{3/2}$
1200	13 581.33*	78.8	7361.04	1.04	$3s\ ^2P_{3/2}-3p\ ^2S_{1/2}$
65	13 544.61		7380.99	0.98	$2p^4\ ^4P_{3/2}-3p\ ^4P_{5/2}$
60	13 534.64	32.7	7386.43	6.43	$^4P_{5/2}-\quad ^4P_{3/2}$
185	13 464.53	62.7	7424.89	4.89	$^4P_{5/2}-\quad ^4P_{5/2}$
21	13 448.12		7433.95	3.95	$3p\ ^2D_{3/2}-4s\ ^2P_{3/2}$
670	13 429.61*	26.1	7444.20	4.20	$3s\ ^2P_{1/2}-3p\ ^2S_{1/2}$
51	12 897.32	98.2	7751.43	1.42	$3p\ ^2D_{5/2}-3d\ ^2P_{3/2}$
5 b l	12 778.5		7823.49	*f*	$3d\ ^2D_{5/2}-5f\ F(4)_{7/2}$
15	12 771.51		7827.78	7.79	$3p\ ^2D_{3/2}-3d\ ^2P_{3/2}$
35	12 730.68		7852.89	2.90	$^2D_{5/2}-\quad ^4F_{7/2}$
30	12 708.89		7866.35	6.35	$^2D_{3/2}-\quad ^2P_{1/2}$
27	12 662.16		7895.39	5.38	$^2D_{3/2}-\quad ^4F_{5/2}$
27	12 581.00	82.3	7946.32	6.31	$^2D_{5/2}-\quad ^2F_{5/2}$
3	12 578.8		7947.73	7.76	$3d\ ^4D_{7/2}-5f\ F(3)_{7/2}$
8	12 575.99		7949.49	*f*	$^4D_{7/2}-\quad F(4)_{9/2}$
4 b l	12 564.4		7956.84	6.81	$^4D_{5/2}-\quad F(3)_{7/2}$
14 u s	12 557.66		7961.09	1.07 1.5**	$3p\ ^2D_{5/2}-3d\ ^4P_{5/2}$ $3d\ ^4D_{3/2}-5f\ F(2)$
6	12 471		8016	6.6**	$3d\ ^2F_{5/2}-5f\ D(3)$
1350	12 469.62*	67.8	8017.30	7.30	$3p\ ^2D_{5/2}-3d\ ^2F_{7/2}$
5 (b l)	12 464.2		8020.80	*f*	$3d\ ^4P_{3/2}-5f\ D(2)_{5/2}$
680	12 461.25*	61.2	8022.68	2.68	$3p\ ^2D_{3/2}-3d\ ^2F_{5/2}$
195	12 438.40	37.7	8037.42	7.43	$^2D_{3/2}-\quad ^4P_{5/2}$
6	12 428.81		8043.62	*f*	$3d\ ^4P_{5/2}-5f\ G(3)_{7/2}$
98	12 404.27	03.1	8059.53	9.52	$3p\ ^4S_{3/2}-3d\ ^2F_{5/2}$
5	12 391.9		8067.56	*f*	$3d\ ^2F_{5/2}-5f\ G(4)_{7/2}$
12	12 384.83		8072.18	*f* 2.05	$^2F_{7/2}-\quad G(5)_{9/2}$ $3p\ ^2D_{3/2}-3d\ ^4P_{3/2}$
375	12 381.65	80.3	8074.26	4.27	$^4S_{3/2}-\quad ^4P_{5/2}$
350	12 328.76	27.7	8108.90	8.89	$^4S_{3/2}-\quad ^4P_{3/2}$
120	12 298.55		8128.82	8.82	$3p\ ^4P_{3/2}-4s\ ^4P_{1/2}$
260	12 288.97	88.0	8135.15	5.01 5.26	$^4P_{5/2}-\quad ^4P_{3/2}$ $3p\ ^4S_{3/2}-3d\ ^4P_{1/2}$
20 b l	12 270.80		8147.20	7.20	$3p\ ^4P_{1/2}-4s\ ^4P_{1/2}$
27 b l	12 261.28		8153.53	3.55	$3p\ ^2D_{5/2}-3d\ ^4D_{7/2}$
11 b l	12 250.11		8160.96	*f*	$3d\ ^4F_{7/2}-5f\ G(4)_{9/2}$
75 b l	12 231.32	32.9	8173.50	3.47	$3p\ ^4P_{3/2}-4s\ ^4P_{3/2}$
12 b l	12 210.17		8187.66	*f*	$3d\ ^4F_{9/2}-5f\ G(5)_{11/2}$
150	12 203.93	03.4	8191.84	1.85	$3p\ ^4P_{1/2}-4s\ ^4P_{3/2}$
480	12 186.82	86.9	8203.34	3.33	$^4P_{5/2}-\quad ^4P_{5/2}$

Table 1 (cont.)

Intensity	Wavelength, Å		Wave-number, cm^{-1}		Combination
	This work	Ingram	Obs.	Calc.	
12	12 142.16		8233.51	3.53	$3p\,^4S_{3/2}-3d\,^4D_{1/2}$
170	12 129.97	28.6	8241.79	1.79	$3p\,^4P_{3/2}-4s\,^4P_{5/2}$
35	12 124.60		8245.44	5.43	$3p\,^4S_{3/2}-3d\,^4D_{3/2}$
25 b l	12 109.30		8255.86	5.83	$^2D_{5/2}-\quad ^2D_{3/2}$
45	12 106.59	07.4	8257.71	7.71	$^4S_{3/2}-\quad ^4D_{5/2}$
230	12 074.51	74.1	8279.64	9.66	$^2D_{5/2}-\quad ^2D_{5/2}$
110	11 998.36	97.9	8332.19	2.20	$^2D_{3/2}-\quad ^2D_{3/2}$

(300 per mm) and a blaze at 20000 Å, and another with 77000 grooves (600 per mm) and a blaze at 16000 Å. The focal length of the parabolic mirrors is one metre. The wavelengths are determined by means of a wave-number scale, which essentially consists of white-light fringes from a Fabry–Perot interferometer. The scale is calibrated by using internationally adopted standards and other well-known lines from the rare-gas spectra. By this method an accuracy of ± 0.02 Å is achieved.

The following two examples from Table 1 may serve as an illustration of the resolution achieved. At 13588 Å two lines with a wavelength difference of 0.83 Å are clearly resolved, and the wavelengths are determined as accurately as for single lines. The line at 18210 Å was seen to consist of two components but could not be resolved. The calculated wavelength difference is in this case 0.33 Å.

Several nitrogen lines fall in regions where the water vapour has strong absorption bands. These lines were recorded with dry air in the spectrograph in order to avoid interference with the water vapour lines.

The observations

The wavelengths of 113 lines from 18751 Å to 11998 Å are given in Table 1. Wavelengths marked with an asterisk are mean values from hollow-cathode and high-frequency discharge measurements, while all other lines have been measured with the latter type of excitation only. The two series of recordings gave the same results within the accidental errors of measurement. For most wavelengths given with two decimal places the uncertainty is estimated to be less than 0.02 Å, but may amount to 0.05 Å for a few lines around 18000 Å. The level combinations have been identified for all lines as shown in the last column in Table 1. Wave-numbers calculated from the final level values are given in column 5 for comparison with the observed values.

In the first column of Table 1 relative intensities are given on a linear scale. They have been evaluated from survey records and roughly corrected with reference to the spectral response of the detector and the blaze properties of the gratings.

Around 12300 Å there is a very strong band of N_2, viz. the 0–1 band of the first positive system (see, for instance, Hepner and Herman, 1957). At an early stage of the present investigation only those lines that clearly rose above the background of band lines were measured. The possibility was still open that some peaks of the background could belong to the N I spectrum, and also that some strong band lines

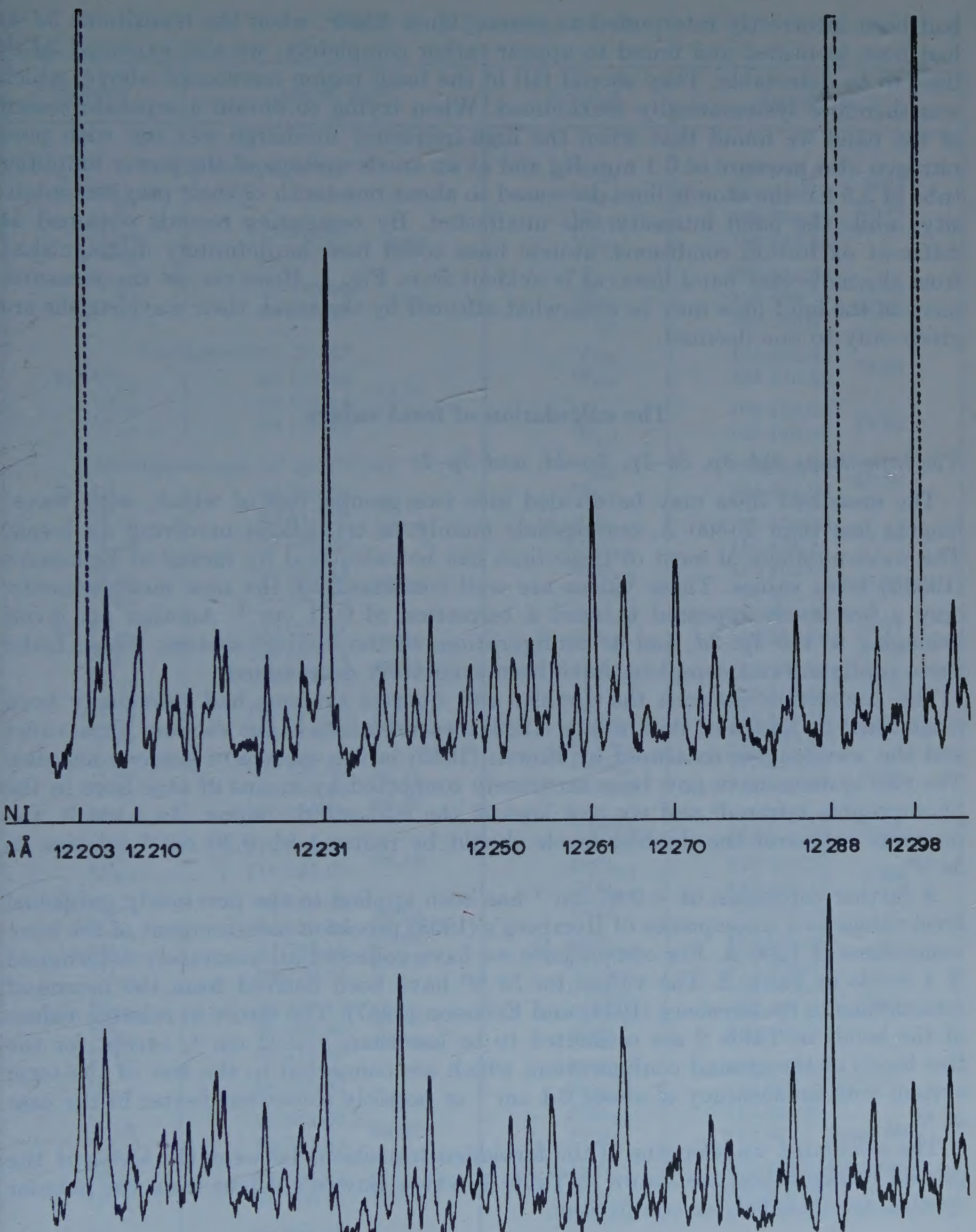

Fig. 1. Nitrogen spectrum from an electrodeless discharge at different excitation conditions, showing atomic and molecular lines.

had been incorrectly interpreted as atomic lines. Later, when the transitions $3d$–$4f$ had been identified and found to appear rather completely, we also expected $3d$–$5f$ lines to be detectable. They should fall in the band region mentioned above, which was therefore systematically reexamined. When trying to obtain a separate record of the band we found that when the high-frequency discharge was run with pure nitrogen at a pressure of 0.1 mm Hg and at an anode voltage of the power amplifier tube of 2.5 kV the atomic lines decreased to about one-tenth of their previous intensity, while the band intensity was unaffected. By comparing records obtained at different excitation conditions, atomic lines could now be definitely distinguished from the molecular band lines, as is evident from Fig. 1. However, as the measurement of the faint lines may be somewhat affected by the band, their wavelengths are given only to one decimal.

The calculation of level values

The transitions $2p^4$–$3p$, $3s$–$3p$, $3p$–$3d$, and $3p$–$4s$

The measured lines may be divided into two groups, one of which, with wavelengths less than 15800 Å, corresponds mainly to transitions involving $3p$ levels. The wave-numbers of most of these lines can be calculated by means of Eriksson's (1958*a*) term values. These values are well confirmed by the new measurements; only a few levels appeared to need a correction of 0.01 cm^{-1}. Another six levels belonging to the $3p$, $3d$, and $4s$ configurations of the doublet system, which make these configurations complete, have been accurately determined.

The connection between the doublet and quartet systems had previously been established by means of Wilkinson's (1955) measurements in the vacuum ultra-violet and the wavelengths measured by Bowen (1955) in the spectra of gaseous nebulae. The two systems have now been accurately connected by means of nine lines in the photographic infrared[1] and six new lines in the lead-sulfide region. As a result, the previous values of the doublet levels should be reduced by 0.36 cm^{-1} relative to $3s\ {}^4P_{1/2}$.

A further correction of $+0.07$ cm^{-1} has been applied to the previously published level values as a consequence of Herzberg's (1958) precision measurement of the resonance lines at 1200 Å. For convenience we have collected all accurately determined N I levels in Table 2. The values for $5s\ {}^4P$ have been derived from the means of measurements by Herzberg (1958) and Eriksson (1957). The errors in relative values of the levels in Table 2 are estimated to be less than ± 0.02 cm^{-1}, except for the five levels of the ground configuration, which are connected to the rest of the term system with an accuracy of about 0.1 cm^{-1} or possibly somewhat better in the case of ${}^4S_{3/2}$.

The calculated wavelengths of the forbidden transitions between the levels of the ground configuration are shown in Table 3, where Bowen's values from the nebular spectra are included for comparison.

The transitions $3d$–nf

A second group of lines, falling beyond 17200 Å, originates from $3d$–$4f$ transitions. The configuration $4f$ consists of 18 levels grouped in nine very narrow pairs, the

---

[1] Including 9020.68 Å, which may now be identified as $3p\ {}^2S_{1/2}$–$3d\ {}^4F_{3/2}$.

Table 2. N I, energy levels.

Symbol	Level, cm⁻¹	
Configuration: $2s^2\,2p^3$		
$2p^3\ {}^4S_{3/2}$	0.00	
${}^2D_{5/2}$	19 223.97	– 8.86
${}^2D_{3/2}$	19 232.83	
${}^2P_{3/2}$	28 839.09	0.28
${}^2P_{1/2}$	28 838.81	
Configuration: $2s\,2p^4$		
$2p^4\ {}^4P_{5/2}$	88 107.23	– 43.91
${}^4P_{3/2}$	88 151.14	– 19.40
${}^4P_{1/2}$	88 170.54	
Configurations: $2s^2\,2p^2\,({}^3P)\,nl$		
$3s\ {}^4P_{5/2}$	83 364.59	46.79
${}^4P_{3/2}$	83 317.80	33.76
${}^4P_{1/2}$	83 284.04	
${}^2P_{3/2}$	86 220.48	83.16
${}^2P_{1/2}$	86 137.32	
$4s\ {}^4P_{5/2}$	103 735.45	68.32
${}^4P_{3/2}$	103 667.13	44.65
${}^4P_{1/2}$	103 622.48	
${}^2P_{3/2}$	104 221.60	76.81
${}^2P_{1/2}$	104 144.79	
$5s\ {}^4P_{5/2}$	109 926.63	70.14
${}^4P_{3/2}$	109 856.49	44.29
${}^4P_{1/2}$	109 812.20	
${}^2P_{3/2}$	110 103.83	68.16
${}^2P_{1/2}$	110 035.67	
$3p\ {}^4D_{7/2}$	94 881.79	50.93
${}^4D_{5/2}$	94 830.86	37.40
${}^4D_{3/2}$	94 793.46	22.61
${}^4D_{1/2}$	94 770.85	
${}^4P_{5/2}$	95 532.12	38.46
${}^4P_{3/2}$	95 493.66	18.38
${}^4P_{1/2}$	95 475.28	
${}^4S_{3/2}$	96 750.81	
${}^2D_{5/2}$	96 864.02	76.37
${}^2D_{3/2}$	96 787.65	
${}^2P_{3/2}$	97 805.81	35.66
${}^2P_{1/2}$	97 770.15	
${}^2S_{1/2}$	93 581.52	
$5p\ {}^2D_{5/2}$	111 905.51	52.54
${}^2D_{3/2}$	111 852.97	
$3d\ {}^4F_{9/2}$	104 765.74	48.82
${}^4F_{7/2}$	104 716.92	33.89
${}^4F_{5/2}$	104 683.03	18.93
${}^4F_{3/2}$	104 664.10	
${}^4D_{7/2}$	105 017.57	9.05
${}^4D_{5/2}$	105 008.52	12.28
${}^4D_{3/2}$	104 996.24	11.90
${}^4D_{1/2}$	104 984.34	
${}^4P_{5/2}$	104 825.08	– 34.62
${}^4P_{3/2}$	104 859.70	– 26.37
${}^4P_{1/2}$	104 886.07	
${}^2F_{7/2}$	104 881.32	70.99
${}^2F_{5/2}$	104 810.33	
${}^2D_{5/2}$	105 143.68	23.83
${}^2D_{3/2}$	105 119.85	
${}^2P_{3/2}$	104 615.44	– 38.56
${}^2P_{1/2}$	104 654.00	
$4f\ G(5)_{11/2}$	110 473.06	– 0.15
$G(5)_{9/2}$	110 473.21	
$G(4)_{9/2}$	110 402.06	– 0.09
$G(4)_{7/2}$	110 402.15	
$G(3)_{7/2}$	110 385.33	0.07
$G(3)_{5/2}$	110 385.26	
$F(4)_{9/2}$	110 501.65	– 0.15
$F(4)_{7/2}$	110 501.80	
$F(3)_{7/2}$	110 498.39	– 0.01
$F(3)_{5/2}$	110 498.40	
$F(2)_{5/2}$	110 486.01	0.08
$F(2)_{3/2}$	110 485.93	
$D(3)_{7/2}$	110 349.14	0.08
$D(3)_{5/2}$	110 349.06	
$D(2)_{5/2}$	110 404.52	0.05
$D(2)_{3/2}$	110 404.47	
$D(1)$	110 459.76	
$5f\ G(5)_{11/2}$	112 953.40	– 0.10
$G(5)_{9/2}$	112 953.50	
$G(4)_{9/2}$	112 877.88	– 0.01
$G(4)_{7/2}$	112 877.89	
$G(3)_{7/2}$	112 868.70	
$F(4)_{9/2}$	112 967.06	– 0.11
$F(4)_{7/2}$	112 967.17	
$F(3)_{7/2}$	112 965.33	
$F(2)$	112 957.7	Predicted
$D(3)$	112 826.9	Predicted
$D(2)_{5/2}$	112 880.50	
$D(1)$	112 946.6	Predicted
Configurations: $2s^2\,2p^2\,({}^1D)\,nl$		
$3s'\ {}^2D_{5/2}$	99 663.33	– 0.50
${}^2D_{3/2}$	99 663.83	
$3p'\ {}^2F_{7/2}$	110 715.06	4.40
${}^2F_{5/2}$	110 710.66	

Table 2 (cont.)

Symbol	Level, cm^{-1}		Symbol	Level, cm^{-1}	
$3p'\,^2D_{5/2}$	110 544.76	23.79	$3d'\,^2G_{9/2}$	120 149.15	$-$ 0.10
$^2D_{3/2}$	110 520.97		$^2G_{7/2}$	120 149.25	
$^2P_{3/2}$	112 319.71	25.78	$4f'\ H(5)$	125 688.0	
$^2P_{1/2}$	112 293.93		Configuration: $2s^2\,2p^2\,(^1S)\,3s$		
			$3s''\,^2S_{1/2}$	116 278.54	

Table 3. Wavelengths of forbidden transitions in N I.

Combination	$\lambda_{\text{calc.}}$, Å	$\lambda_{\text{obs.}}$	Reference
$2p^3\,^2D_{3/2}$–$2p^3\,^2P_{1/2}$	10 407.33 ± 0.2		
$^2D_{3/2}$– $^2P_{3/2}$	10 407.03 ± 0.2		
$^2D_{5/2}$– $^2P_{1/2}$	10 397.74 ± 0.2		
$^2D_{5/2}$– $^2P_{3/2}$	10 397.44 ± 0.2		
$^4S_{3/2}$– $^2D_{5/2}$	5 200.39 ± 0.05	0.41 ± 0.1	Bowen (1955)
$^4S_{3/2}$– $^2D_{3/2}$	5 198.00 ± 0.05	7.94 ± 0.1	
$^4S_{3/2}$– $^2P_{1/2}$	3 466.58 ± 0.03	6.38 ± 0.3	Bowen (1960)
$^4S_{3/2}$– $^2P_{3/2}$	3 466.55 ± 0.03		

splitting of which is less than 0.2 cm^{-1}. Naturally, it has not been possible to resolve transitions from the two levels of a $4f$ pair to the same $3d$ level, but several of the individual $4f$ levels could be determined from theoretically unblended transitions. In other cases an estimation of the expected relative intensities in a mixed transition and an examination of line profiles helped in determining the separate levels of a pair. However, for some $4f$ pairs the centre of gravity is better defined than the separate levels.

The lines observed of the transition $3d$–$5f$ were too few to permit a definite identification from the observations alone. Here, however, a theoretical prediction (cf. next section) proved to be so successful that the identifications could be made without ambiguity.

Pair-coupling theory of the $2s^2\,2p^2\,nf$ configurations

As has already been mentioned the $(^3P)\,4f$ configuration consists of nine pairs with very narrow splittings. A look at the $3d$–$4f$ transition array in Table 4, showing the observed intensities, makes the diagonal character evident. Consequently, L is a useful quantum number for this configuration, which implies a strong electrostatic interaction between the core and the f electron. The pairs are obtained by a coupling of L with the spin of the core to a resultant K. It is only the pairs $4f\ G(3)$ and $4f\ D(3)$ that give rise to strong off-diagonal transitions, indicating an exchange of characteristics between these two pairs. However, these transitions are partly due to the properties of the $3d$ configuration, in particular the mixing of $^4P_{5/2}$ with $^2F_{5/2}$.

Table 4. Relative intensities of the transitions $3d$–$4f$. The parentheses indicate coincident transitions.

	$4f$	$G(5)$		$G(4)$		$G(3)$		$F(4)$		$F(3)$		$F(2)$		$D(3)$		$D(2)$		$D(1)$	
$3d$	J	11/2	9/2	9/2	7/2	7/2	5/2	9/2	7/2	7/2	5/2	5/2	3/2	7/2	5/2	5/2	3/2	3/2	1/2
^4F	9/2	125						16											
^2F	7/2		(100)^1	12					8										
^4F	7/2		23	(100)^2		8		4		6									
^2F	5/2				(100)^1									(33)					
^4F	5/2				27	18								42					
^4F	3/2						32								(100)^2				
^4D	7/2			4				60		13				2					
^2D	5/2								32	4		11							
^4D	5/2								8	(32)^3									
^2D	3/2										13	13							
^4D	3/2										13	(32)^3							
^4D	1/2												13						
^4P	5/2				8	51								10		7			
^2P	3/2						16								24	11			
^4P	3/2															30		10	
^2P	1/2																12	10	
^4P	1/2																6	17	

Table 5. The configuration p^2f in the pair-coupling approximation.

Limit	L	K	Energy value
$^1S_0$	F	3	$E_0+(^1S)-(^3P)$
$^1D_2$	H	5	$E_0+(^1D)-(^3P)+10F_2$
$^1D_2$	G	4	$E_0+(^1D)-(^3P)-15F_2$
$^1D_2$	F	3	$E_0+(^1D)-(^3P)-11F_2$
$^1D_2$	D	2	$E_0+(^1D)-(^3P)+\ 6F_2$
$^1D_2$	P	1	$E_0+(^1D)-(^3P)+24F_2$
$^3P_2$	G	5	$E_0+\frac{1}{3}A+\frac{1}{9}B-\ 5F_2$
$^3P_2$	D	1	$E_0+\frac{1}{3}A+\frac{1}{9}B-12F_2$
$^3P_2$	F	4	$E_0-\frac{1}{6}A+\frac{1}{9}B+5F_2\pm[(\frac{1}{2}A)^2+\frac{5}{2}AF_2+(10F_2)^2]^{\frac{1}{2}}$
$^3P_1$	G	4	
$^3P_2$	F	2	$E_0-\frac{1}{6}A+\frac{1}{9}B+\frac{3}{2}F_2\pm[(\frac{1}{2}A)^2-\frac{9}{2}AF_2+(\frac{27}{2}F_2)^2]^{\frac{1}{2}}$
$^3P_1$	D	2	
$^3P_2$	F	3	$E_0\qquad-\frac{2}{9}B-\frac{2}{3}F_2+x_i$
$^3P_1$	G	3	
$^3P_0$	D	3	

$A=(^3P_2)-(^3P_1)$, $B=(^3P_2)-(^3P_0)$, $F_2=F_2(p,f)$.
x_i are the roots of the equation $x^3-px=q$ with

$$3p=A^2+B^2-AB+(\tfrac{41}{2}A-2B)F_2+589F_2^2$$
$$27q=-2A^3-2B^3+3A^2B+3AB^2+(-\tfrac{123}{2}A^2+6B^2+111AB)F_2+ \\ +(1362A+282B)F_2^2+20774F_2^3.$$

The structure of p^2f in intermediate pair coupling has been theoretically treated by Eriksson (1961) in connection with this investigation. The resulting formulae, reproduced in Table 5, contain as adjustable parameters only the electrostatic coupling parameter $F_2(2p, nf)$ and the energy E_0 of the centroid of the configuration $(^3P)nf$. The remaining constants of the formulae are the differences between the parent levels, which are obtained to a good approximation from the observations in N II (Eriksson, 1958*b*).

Table 6 gives a comparison between observed and calculated values of the $4f$ and $5f$ pairs. The agreement for $4f$ confirms the validity of the theory and supports the classification of the $3d$–$5f$ transitions. In the latter case the experimental classification was difficult because the observed lines were few and of low intensity. When judging the agreement, it should be remembered that the accepted intervals of N II $2p\ ^3P$ are known with an accuracy of 0.1 to 0.2 cm^{-1} only.

The $4f'$ and $4f''$ levels, based on the parent terms $^1D_2$ and $^1S_0$ in N II, fall above the (^3P) limits, and most of them are subject to autoionization. For $4f'$ $H(5)$, which should not be autoionized, a term value of 125688.3 cm^{-1} is predicted by using the value 15227.3 cm^{-1} for (^1D)–(^3P) in the second formula of Table 5. The strongest transition from this pair should be $3d'\ ^2G$–$4f'\ H(5)$ with a predicted wave-number of 5539.1 ± 0.5 cm^{-1}, which coincides with the transition $3d\ ^2F_{5/2}$–$4f\ D(3)$. The observed line 5538.79 cm^{-1} is probably a blend including both transitions.

Table 6. N I $2s^2 2p^2(^3P)nf$. Centres of gravity of the pairs, as observed and calculated from the formulae of Table 5. E_0, the centroid of the $(^3P)nf$ configuration, and F_2, the electrostatic $(2p, nf)$ interaction parameter, have been treated as adjustable parameters.

$L(K)$	$4f$			$5f$		
	Calc., cm^{-1}	Obs.	Obs. − calc.	Calc., cm^{-1}	Obs.	Obs. − calc.
$F(4)$	110 501.72	1.72	0.00	112 967.15	7.11	−0.04
$F(3)$	110 498.35	8.39	0.04	112 965.31	5.33	0.02
$F(2)$	110 485.88	5.98	0.10	112 957.74		
$G(5)$	110 473.37	3.13	−0.24	112 953.59	3.45	−0.14
$D(1)$	110 459.62	9.76	0.14	112 946.59		
$D(2)$	110 404.32	4.50	0.18	112 880.34	0.50	0.16
$G(4)$	110 402.23	2.10	−0.13	112 877.93	7.88	−0.05
$G(3)$	110 385.30	5.30	0.00	112 868.65	8.70	0.05
$D(3)$	110 349.12	9.11	−0.01	112 826.91		
E_0	110 441.30 cm^{-1}			112 916.69 cm^{-1}		
A	82.10 cm^{-1}			82.10 cm^{-1}		
B	130.80 cm^{-1}			130.80 cm^{-1}		
F_2	1.965 cm^{-1}			1.000 cm^{-1}		
$n^3 \times F_2$	125.76 cm^{-1}			125.0 cm^{-1}		

The formulae of Table 5 permit an accurate determination of the structures of higher nf-configurations because of the fact that the product $n^3 \times F_2$ appears to be practically constant. As a knowledge of $6f$ would be sufficient for calculating the ionization limit by means of a Ritz formula, a measurement of the transitions $3d$–$6f$ would be of interest. This line group should fall between 10000 Å and 11000 Å in the strong 0–0 band of the first positive system of N_2, but it might be possible to separate the atomic lines from molecular band lines by means of a large-dispersion spectrograph now available in this laboratory.

ACKNOWLEDGEMENTS

To Professor Bengt Edlén the authors are indebted for sustained interest and invaluable advice. We are also grateful to Fil. Dr. Lennart Stigmark for helpful consultations in electronics and to Fil. Mag. Sixten Hvalgren for measuring many of the records.

Department of Physics, University of Lund.

REFERENCES

Bowen, I. S., Astrophys. J. *121,* 306 (1955).
—— Astrophys. J. *132,* 1 (1960).
Eriksson, K. B. S., unpublished measurements (1957).
—— Arkiv Fysik *13,* 429 (1958*a*).
—— Arkiv Fysik *13,* 303 (1958*b*).
—— Arkiv Fysik *19,* 229 (1961).

ERIKSSON, K. B. S., and JOHANSSON, I., Arkiv Fysik *16*, 490 (1960).
HEPNER, G., and HERMAN, L., Ann. géophys. *13*, 242 (1957).
HERZBERG, G., Proc. Roy. Soc. London *A 248*, 309 (1958).
INGRAM, S. B., Phys. Rev. *34*, 421 (1929).
JOHANSSON, I., Arkiv Fysik *15*, 169 (1959).
MINNHAGEN, L., and STIGMARK, L., Arkiv Fysik *8*, 471 (1954).
WILKINSON, P. G., J. Opt. Soc. Amer. *45*, 862 (1955).

Tryckt den 18 mars 1961

Uppsala 1961. Almqvist & Wiksells Boktryckeri AB